Proceedings of the 2001 IEEE/RSJ
International Conference on Intelligent Robots and Systems
Maui, Hawaii, USA, Oct. 29 - Nov. 03, 2001

An Extended Kalman Filter for Quaternion-Based Orientation Estimation Using MARG Sensors

João Luís Marins[1], Xiaoping Yun[2], Eric R. Bachmann, Robert B. McGhee, and Michael J. Zyda
Naval Postgraduate School
Monterey, CA 93943

Abstract: This paper presents an extended Kalman filter for real-time estimation of rigid body orientation using the newly developed MARG (Magnetic, Angular Rate, and Gravity) sensors. Each MARG sensor contains a three-axis magnetometer, a three-axis angular rate sensor, and a three-axis accelerometer. The filter represents rotations using quaternions rather than Euler angles, which eliminates the long-standing problem of singularities associated with attitude estimation. A process model for rigid body angular motions and angular rate measurements is defined. The process model converts angular rates into quaternion rates, which are integrated to obtain quaternions. The Gauss-Newton iteration algorithm is utilized to find the best quaternion that relates the measured accelerations and earth magnetic field in the body coordinate frame to calculated values in the earth coordinate frame. The best quaternion is used as part of the measurements for the Kalman filter. As a result of this approach, the measurement equations of the Kalman filter become linear, and the computational requirements are significantly reduced, making it possible to estimate orientation in real time. Extensive testing of the filter with synthetic data and actual sensor data proved it to be satisfactory. Test cases included the presence of large initial errors as well as high noise levels. In all cases the filter was able to converge and accurately track rotational motions.

1. Introduction

Accurate real-time tracking of orientation or attitude of rigid bodies has wide applications in robotics, aerospace, underwater vehicles, automotive industry, virtual reality, and others. A number of motion tracking technologies have been developed for virtual reality applications, including mechanical trackers, active magnetic trackers, optical tracking systems, acoustic tracking systems, and inertial tracking systems.

Mechanical trackers can be placed in two separate categories. Body-based systems utilize an exoskeleton that is attached to the articulated structure to be tracked. Goniometers within the skeletal linkages measure joint angles. Ground-based systems attach one end of a boom or shaft to an object to be tracked and typically have six degrees of freedom [1].

Active magnetic tracking systems determine both position and orientation by using small sensors mounted on a rigid body to sense a set of generated magnetic fields. The sensors contain three mutually perpendicular coils. Changes in strength across the coils are proportional to the distance of each coil from the field emitter assembly. Three sequentially emitted fields create one induced current in each of the three sensor coils, allowing measurement of orientation [2].

Practical optical tracking systems may be separated into two basic categories. *Pattern recognition systems* sense an artificial pattern of lights and use this information to determine position and/or orientation. [3] *Image-based systems* determine position by using multiple cameras to track predesignated points on moving objects within a working volume. The tracked points may be marked actively or passively [4].

Ultrasonic tracking systems can determine position through either time-of-flight and triangulation or phase-coherence. Phase-coherence trackers determine distance by measuring the difference in phase of a reference signal and an emitted signal detected by sensors.

Fuchs (Foxlin) presented an inertial system for head tracking applications [5]. This system utilized a fluid pendulum and three solid-state piezoelectric angular rate sensors. More recent publications describe the use of three orthogonal solid-state rate gyros, a two-axis fluid inclinometer and a two-axis fluxgate compass [6]. Sensor data is processed by a complementary separate-bias Kalman filter.

[1] Current Address: Brazilian Navy Research Institute, Rua Ipiru 2, Jardim Guanabara, Rio de Janeiro, RJ, Brazil, 21.931-090, Email: jlmarins@hotmail.com.
[2] Correspondence Address: Department of Electrical and Computer Engineering, Code EC/Yx, Naval Postgraduate School, Monterey, CA 93943, USA, Email: yun@nps.navy.mil.

Hayward et al. [7] presents an attitude tracking system with GPS and inertial sensors used for aircraft. The difference among the GPS signals received by three antennas gives attitude information. Quine [8] replaces the antenna information with information coming from celestial observations. Leader [9] describes an attitude package, which combines the outputs of inclinometers, gyros, and compasses to obtain attitude estimation. All three examples utilize Euler angles to represent orientation and a Kalman filtering algorithm to integrate the information.

Bachmann et al. [10] presented a motion tracking system that is based the MARG (Magnetic, Angular Rate, and Gravity) sensors. MARG sensors are hybrid inertial and magnetic sensors. Each MARG sensor contains a three-axis magnetometer, a three-axis angular rate sensor, and a three-axis accelerometer mounted in a "strapdown" configuration. Quaternions are used to represent orientations. The use of quaternions avoids the singularity problem, characteristic of filters that use Euler angles. A constant-gain complementary filter was developed to estimate the attitude of a rigid body that a MARG sensor is attached to.

This paper follows the same approach of [10], but replaces the complementary filter with a Kalman filter. The use of quaternions is maintained because of characteristics that make them very suitable for this approach. They can easily be transformed into a matrix and can be integrated easily due to their dependence on the angular rates. An innovative Kalman filter design is described, which reduces the order of the output vector as well as the computational effort needed to run the filter. Testing results using synthetical data and actual sensor data are presented.

2. Quaternions

Orientation can be defined as a set of parameters that relates the angular position of a frame to another reference frame. There are numerous methods for describing this relation. Some are easier to visualize than others are. Each has some kind of limitations. Among them, rotation matrices, Euler angles and quaternions are commonly used. Orientation or attitude tracking systems continuously estimate the angular parameters of a body based on certain measurement

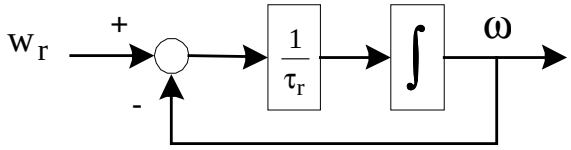

Figure 1. Process Model for Angular Rates.

data. Quaternions are a four-dimensional extension to complex numbers. A quaternion can be regarded as an element of $\Re^4$. In this paper, quaternions will be represented using the notation from [11]:

$$n = a\,i + b\,j + c\,k + d = \vec{n} + n_0 \qquad (1)$$

where *a*, *b*, *c*, and *d* are real numbers and *i*, *j*, and *k* are unit vectors directed along the *x*, *y*, and *z* axis respectively. A quaternion is a unit quaternion if

$$n_0 = \cos\theta \quad \text{and} \quad |\vec{n}| = \sin\theta \qquad (2)$$

for some angle θ. Unit quaternions can be used to rotate a vector $\vec{u}$. The rotation is performed through the double quaternion multiplication [12]

$$\vec{v} = n\,\vec{u}\,n^* \qquad (3)$$

where n^* is the complex conjugate of the quaternion n defined as

$$n^* = -a\,i - b\,j - c\,k + d \qquad (4)$$

This operation rotates the vector $\vec{u}$ through an angle 2θ about the axis defined by $\vec{n}$. The operation using Equation (3) is equivalent to a matrix multiplication

$$\vec{v} = n\,\vec{u}\,n^* = R\,\vec{u} \qquad (5)$$

where, providing n is a unit quaternion,

$$R = \begin{bmatrix} d^2+a^2-b^2-c^2 & 2(a\,b-c\,d) & 2(a\,c+b\,d) \\ 2(a\,b+c\,d) & d^2+b^2-a^2-c^2 & 2(b\,c-a\,d) \\ 2(a\,c-b\,d) & 2(b\,c+a\,d) & d^2+c^2-b^2-a^2 \end{bmatrix} \qquad (6)$$

3. Process Model

To design a Kalman filter for estimating orientation, the first step is to develop a process model of a rigid body under rotational motion [13]. Let the angular rate ω of the rigid body be defined as:

p: body angular velocity around the *x* axis (roll),
q: body angular velocity around the *y* axis (pitch),
r: body angular velocity around the *z* axis (yaw).

The state vector of a process model will consists of the angular rate ω and parameters for characterizing

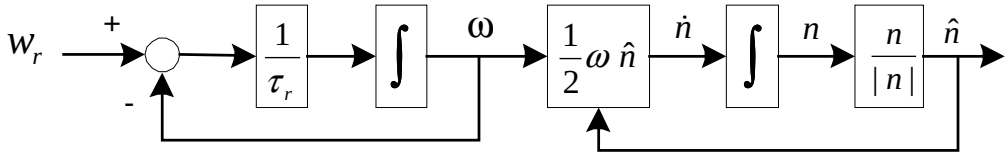

Figure 2. Process Model for Angular Rates and Quaternions.

orientation, in this case, quaternion *n*. For human body motions, it is shown in [10] that a simple first order model for the angular rate as shown in Figure 1 is sufficient. In the diagram

- w_r is a 3-dimensional vector representing white noise sequences with known covariance that generate *p*, *q*, and *r*,
- τ_r is the time constant for *p*, *q*, and *r*, and
- ω represents the angular rates *p*, *q*, and *r*.

The variances of the white sequences and the time constants are to adjusted so that the spectral characteristics of the signal generated by the model match those of the angular rates under normal operational conditions.

Quaternion rates are related to angular rates through the following simple quaternion product [12]:

$$\dot{n} = \frac{1}{2}\, n\, \omega \tag{7}$$

In the equation above, ω is treated as a quaternion with zero scalar part.

Combining Equation (7) with the angular rate model depicted in Figure 1, we obtain a complete model of a rigid body for the purpose of estimating its rotational motions. The complete model is shown in Figure 2. It is noted that the quaternion resulted from the integration is normalized by

$$\hat{n} = \frac{n}{|n|} \tag{8}$$

This is because unit quaternions are needed justify the use of Equation (6) to perform vector rotations as discussed above.

4. Kalman Filter Design

In this section, two approaches to the Kalman filter design are described. The first approach is a standard one, which has seven states (3-dimensional angular rates, and 4-dimensional quaternion), and nine outputs (nine measurements directly from the MARG sensor). It turns out that the output equations are highly nonlinear, and the resultant extended Kalman filter becomes very complicated, making it difficult to implement in real time. A second approach is thus proposed. This approach uses the Gauss-Newton iteration algorithm to find the best matched quaternion for each measurement from the accelerometers and magnetometers. The computed quaternion from the Gauss-Newton iteration algorithm is taken as part of measurements for the Kalman filter, in addition to the measurements provided by the angular rate sensor. As a result, the outputs of the Kalman filter are reduced from nine to seven. More importantly, the output equations become linear, which greatly simplifies the design of the filter. The feasibility of this approach heavily relies on fast convergence of the Gauss-Newton iteration algorithm. Extensive simulations show that the iteration algorithm converges in just 3 to 4 steps, which ensures the success of this alternative approach.

4.1 The First Approach

As was discussed earlier, the states of the process model are:

- x_1 : angular rate *p*
- x_2 : angular rate *q*
- x_3 : angular rate *r*
- x_4 : quaternion component *a*
- x_5 : quaternion component *b*
- x_6 : quaternion component *c*
- x_7 : quaternion component d (scalar component)

Based on the model from Figure 2, the state equations can be written as

$$\dot{x}_1 = -\frac{1}{\tau_{rx}} x_1 + \frac{1}{\tau_{rx}} w_{rx} \tag{9}$$

$$\dot{x}_2 = -\frac{1}{\tau_{ry}} x_2 + \frac{1}{\tau_{ry}} w_{ry} \tag{10}$$

$$\dot{x}_3 = -\frac{1}{\tau_{rz}} x_3 + \frac{1}{\tau_{rz}} w_{rz} \tag{11}$$

$$\dot{x}_4 = \frac{1}{2\sqrt{x_4^{\,2} + x_5^{\,2} + x_6^{\,2} + x_7^{\,2}}} (x_3 x_5 - x_2 x_6 + x_1 x_7) \tag{12}$$

$$\dot{x}_5 = \frac{1}{2\sqrt{x_4^{\,2} + x_5^{\,2} + x_6^{\,2} + x_7^{\,2}}}(-x_3 x_4 + x_1 x_6 + x_2 x_7) \tag{13}$$

$$\dot{x}_6 = \frac{1}{2\sqrt{x_4^{\,2} + x_5^{\,2} + x_6^{\,2} + x_7^{\,2}}}(x_2 x_4 - x_1 x_5 + x_3 x_7) \tag{14}$$

$$\dot{x}_7 = \frac{1}{2\sqrt{x_4^{\,2} + x_5^{\,2} + x_6^{\,2} + x_7^{\,2}}}(-x_1 x_4 - x_2 x_5 - x_3 x_6) \tag{15}$$

It is noted that the product terms in the parentheses are introduced by quaternion product between the angular rate and the quaternion, and the square-root terms appeared in the denominator are due to the quaternion normalization.

Since measurement data to the filter are provided by the MARG sensor, it is natural to choose the following as the outputs of the Kalman filter:

z_1 : angular rate *p*

z_2 : angular rate *q*

z_3 : angular rate *r*

z_4 : component of gravity on the *x*-axis of the body frame

z_5 : component of gravity on the *y*-axis of the body frame

z_6 : component of gravity on the *z*-axis of the body frame

z_7 : component of the local magnetic field on the *x*-axis of the body frame

z_8 : component of the local magnetic field on the *y*-axis of the body frame

z_9 : component of the local magnetic field on the *z*-axis of the body frame

Since angular rates are part of the state, the first three output equations are linear and fairly simple:

$$z_1 = x_1 \tag{16}$$

$$z_2 = x_2 \tag{17}$$

$$z_3 = x_3 \tag{18}$$

As for the remaining six output equations, they turn out to be quite complicated. As an example, the fourth output equation is given by:

$$z_4 = ((x_4^2 + x_7^2 - x_5^2 - x_6^2)h_1 + 2(x_4 x_5 - x_6 x_7)h_2 + 2(x_4 x_6 + x_5 x_7)h_3)/(x_4^2 + x_5^2 + x_6^2 + x_7^2) \tag{19}$$

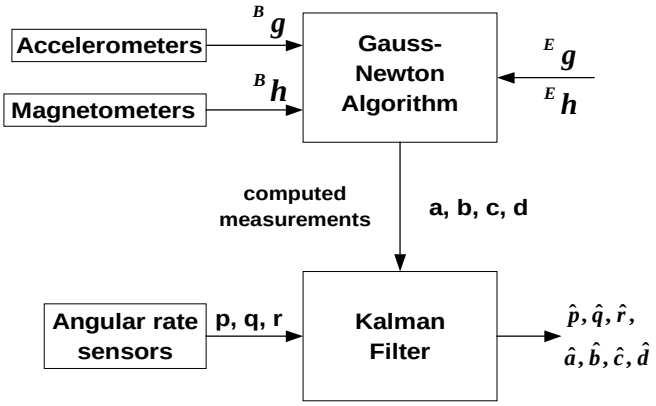

Figure 3. Diagram of the Kalman filter Using the Second Approach.

where h_1, h_2, and h_3 are values of the earth magnetic field measured in earth coordinates, which are constant for a given location. It is not difficult to design an extended Kalman filter based on the state equations (9) to (15), and the nine output equations, which we did. The problem is that computational requirements for implementing such a filter is extremely high, making it unfeasible for real-time motion tracking since a minimum of fifteen MARG sensors are needed to fully track one avatar, not to mention simultaneous tracking of multiple avatars in a virtual environment. An alternative approach to the Kalman filter design is thus presented in the next two subsections.

4.2. Algorithms For Quaternion Convergence

We first describe two convergence algorithms. Consider a rigid body on which a tri-orthogonal coordinate frame is attached to its center of gravity. If three accelerometers and three magnetometers are fixed to the origin of the frame, they measure components of the gravity and of the earth magnetic field in the axis of the frame as the body rotates. Because these values are known and constant for a given geographic area, one can expect that there exists a quaternion relating the measurements (values in body frame) to the real magnetic and gravity fields (values in earth frame).

Obviously there are several sources of errors, including:

- misalignments between pairs of axes in each sensor;
- linear acceleration misinterpreted as gravity;
- variation of both gravity and magnetic field; and
- errors inherent to the sensors.

As a result, there is not a quaternion that exactly converts what is measured (body frame) into the known values (earth frame). The solution is to determine the best quaternion such that, after the conversion, the error is minimized. This paper examines this problem using the minimum-squared-error (MSE) criterion. It is noted that error can be minimized in either the body frame or in the earth frame. Error is minimized in the earth frame in this derivation. Two different algorithms are evaluated.

Let Q be the error function defined as

$$ {}^{E}Q = \varepsilon^{T}\varepsilon = ({}^{E}y_1 - M\ {}^{B}y_0)^{T}\ ({}^{E}y_1 - M\ {}^{B}y_0) \qquad (20) $$

where

${}^{E}y_1$: is a 6x1 vector with values of gravity and magnetic field in the earth frame,

${}^{B}y_0$: is a 6x1 vector with the measurements of gravity and magnetic field in the body frame,

and

$$ M = \begin{bmatrix} R & 0 \\ 0 & R \end{bmatrix} \qquad (21) $$

The matrix R in Eqation (21) is defined by Equation (6).

Because y_0 is measured and y_1 is known, the error between them is a function of the matrix M, which in turn depends on the four components of the quaternion. The objective is to find iteratively the values of quaternion components that yield the minimum error.

Several optimization algorithms exist in the literature. Among them the Newton and Gauss-Newton algorithms are the most used ones. The main difference between them is that the former uses the first and second derivatives of the error function (gradient and Hessian) and the latter uses only the first derivative (Jacobian), which is related to the gradient.

The formulation for the iterative algorithm can be found in [14]. For the Gauss-Newton method it is given as:

$$ \hat{n}_{k+1} = \hat{n}_k - \left[J^{T}(\hat{n}_k)\, J(\hat{n}_k) \right]^{-1} J^{T}(\hat{n}_k)\ {}^{E}\varepsilon(\hat{n}_k) \qquad (22) $$

where $\hat{n}$ is a vector with the four components of the quaternion and J is the Jacobian matrix defined as

$$ J = -\left[\left(\frac{\partial M}{\partial a}\ {}^{B}y_0\right) \ \left(\frac{\partial M}{\partial b}\ {}^{B}y_0\right) \ \left(\frac{\partial M}{\partial c}\ {}^{B}y_0\right) \ \left(\frac{\partial M}{\partial d}\ {}^{B}y_0\right) \right] \qquad (23) $$

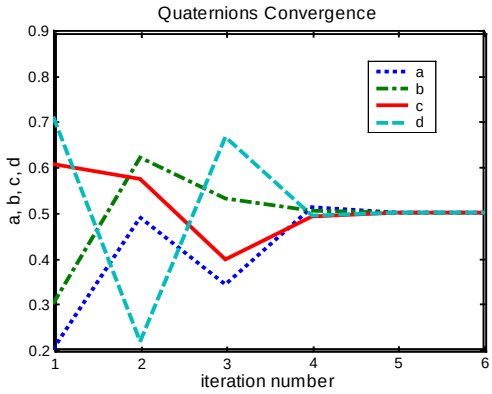

Figure 4. Quaternion Convergence of the Newton Method.

For the Newton method, the algorithm is given as:

$$ \hat{n}_{k+1} = \hat{n}_k - \left[\nabla^{2}{}_{n}\,{}^{E}Q(\hat{n}_k) \right]^{-1} \left[\nabla_{n}\,{}^{E}Q(\hat{n}_k) \right] \qquad (24) $$

where $\nabla_{n}\,{}^{E}Q$ is the gradient of the error function Q calculated in the earth coordinates with respect to each of the four quaternion components. The gradient is calculated using the formula [15]:

$$ \nabla_{n}\,{}^{E}Q = -2 \begin{bmatrix} \left(\frac{\partial M}{\partial a}\ {}^{B}y_0\right)^{T} \\ \left(\frac{\partial M}{\partial b}\ {}^{B}y_0\right)^{T} \\ \left(\frac{\partial M}{\partial c}\ {}^{B}y_0\right)^{T} \\ \left(\frac{\partial M}{\partial d}\ {}^{B}y_0\right)^{T} \end{bmatrix} \left({}^{E}y_1 - M\ {}^{B}y_0\right) \qquad (25) $$

In the same way, the Hessian is the second order derivative of the error function Q calculated in the earth coordinates with respect to the quaternion components. It is calculated by the formula [15]:

$$ \nabla(\nabla_{n}\,{}^{E}Q) = \left\{ \begin{bmatrix} \frac{\partial^2 M}{\partial a^2} & \cdots & \frac{\partial^2 M}{\partial a \partial d} \\ \vdots & & \vdots \\ \frac{\partial^2 M}{\partial d \partial a} & \cdots & \frac{\partial^2 M}{\partial d^2} \end{bmatrix} {}^{B}y_0 \left({}^{E}y_1 - M\,{}^{B}y_0\right) - \begin{bmatrix} \left(\frac{\partial M}{\partial a}\ {}^{B}y_0\right)^{T} \\ \vdots \\ \left(\frac{\partial M}{\partial d}\ {}^{B}y_0\right)^{T} \end{bmatrix} \begin{bmatrix} \left(\frac{\partial M}{\partial a}\ {}^{B}y_0\right)^{T} \\ \vdots \\ \left(\frac{\partial M}{\partial d}\ {}^{B}y_0\right)^{T} \end{bmatrix}^{T} \right\} \qquad (26) $$

The success of the alternative Kalman filter design is dependent completely on convergence of the Gauss or Gauss-Newton method. Fortunately, both methods not only converge, but also converge in 3 or 4 steps in most cases. Convergence results will be presented in Section 5.

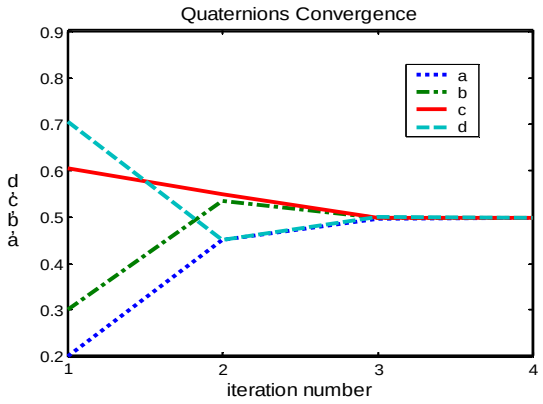

Figure 5. Quaternion Convergence of the Gauss-Newton Method.

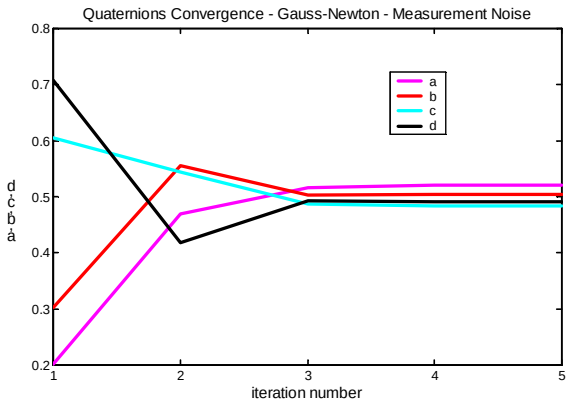

Figure 6. Quaternion Convergence of the Gauss-Newton Method with Measurement Noise.

4.3. The Second Approach

With the introduction of the convergence algorithm as an external loop to the Kalman filter, the quaternion components are now available as measurements. Figure 3 shows the schematic and data flow of the second approach.

The state equations are the same as before, that is, Equations (9)-(15). However, the output equations are different and much simpler. Now the outputs are:

z_1 : angular rate p

z_2 : angular rate q

z_3 : angular rate r

z_4 : quaternion component a

z_5 : quaternion component b

z_6 : quaternion component c

z_7 : quaternion component d

As can be seen, the outputs are exactly the same as the states. Therefore, the output equations are simply identity functions, that is,

$$z_i = x_i \qquad i = 1,...,7$$

Although the output equations are linear, an extended Kalman filter is required since part of the state equations is nonlinear. Nevertheless, linearity in the output equations significantly simplifies the filter design and reduces the computational requirements for real-time implementation.

5. Testing and Simulation Results

In this section, testing and simulation results of the quaternion convergence algorithms and the second approach of the Kalman filter are described.

5.1 Testing of the Convergence Algorithms

The objective of the test is to check the convergence for different rotations, initial estimates, and noise levels. A six-element vector is chosen, which contains the components of gravity and local magnetic field vectors. An arbitrary quaternion is selected and used to rotate the initial vector. Gaussian noise is added to the rotated vector in order to simulate the measurement noise. The initial guesses are chosen to be values around the real value of the quaternion.

Figures 4 and 5 show the result of the Newton and Gauss-Newton algorithms, respectively. In this case, no noise was added. Both algorithms converge in three or four iteration steps. Testing was also conducted with added noise. The algorithms now converge to the best value of quaternion and the error is not zero any more. Figure 6 shows the convergence using the Gauss-Newton algorithm with added noise. Extensive simulation was carried out, and similar results were observed in all cases [15].

The above reported convergence results apply to the cases of large errors in initial estimates. Additional experiments, reported in [16], show that during tracking, when errors are much smaller, Guass-Newton iteration typically converges to sufficient accuracy in only one step.

5.2 Testing of the Complete Kalman Filter

The Kalman filter designed using the second approach was tested with ideal (synthetic) data and actual data collected from a prototype MARG sensor.

The purpose of the test with ideal data is to verify that the filter converges to the correct steady-state values after a single rotation. The ideal data were generated as follow. Both frames are coincident at the beginning and then the body frame was rotated 120

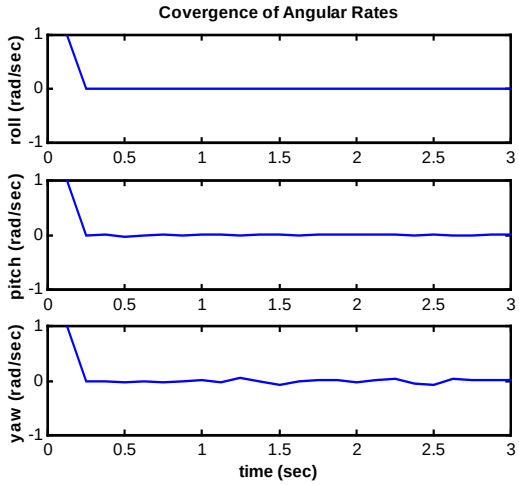

Figure 7. Convergence of Angular Rates Using Ideal Data.

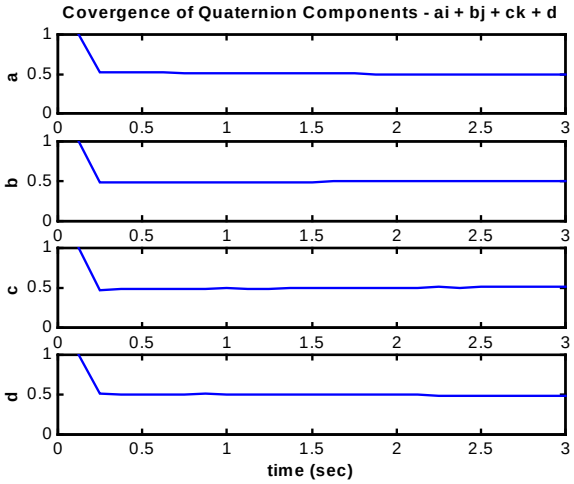

Figure 8. Convergence of Quaternion Components Using Ideal Data.

degrees about the axis $\vec{m} = [1 \quad 1 \quad 1]$. The initial values utilized for the states and the expected steady-state values are listed below:

	p	q	r	a	b	c	d
Initial Values	1.0	1.0	1.0	1.0	1.0	1.0	1.0
Steady State	0	0	0	0.5	0.5	0.5	0.5

The filter results are depicted in Figures 7 and 8. It is seen that both the angular rates and quaternion components converge to the steady state in less than a half of seconds.

The Kalman filter was tested with actual measurement data collected from a MARG sensor as well. During the period when data were collected, the MARG sensor was first rotated 90 degrees about the *x* axis, followed by a 90 degree rotation about the *y* axis, and finally rotated 90 degrees about the *z* axis. Angular rates should be zero except the three brief moments when the sensor was rotated. The tracking results produced by the Kalman filter are presented in Figure 9 and 10. Figure 9 shows the filter tracking result of angular rates. It is seen that each component of angular rates is mostly zero except the brief moment when the sensor was rotated about that axis, as expected. Minor coupling between axes was noticeable. This is because the MARG sensor was rotated by hand against a tabletop. It is difficult to keep other two axes absolutely fixed while rotating about one axis. Figure 10 shows the tracking results of quaternion components. The expected values are marked right above or below each trajectory segment. It is seen that the filter is able to successfully track orientations.

It should be pointed out that testing results presented here are qualitative in nature. More precise and quantitative testing will be conducted using a high-precision turntable in the near future.

7. Conclusions

This paper presented a complete design of an extended Kalman filter for real-time estimation of rigid body motion attitude. The use of quaternions to represent rotations, instead of Euler angles, eliminates the long-standing problem of singularities called "gimbal lock."

Two approaches to the Kalman filter design were investigated. The first approach used nine output equations: three angular rates, three components of linear acceleration, and three components of the earth magnetic field. Since these output equations were highly nonlinear functions of the process state variables, the partial derivatives needed for the Kalman filter design were very complicated. As a result, a filter formulated with these equations would not be useful for real-time applications.

The second approach utilized Gauss-Newton iteration algorithm to find the optimal quaternion that related the measurements of linear accelerations and earth magnetic field in the body coordinate frame to the values in the earth coordinate frame. The optimal quaternion was used as part of the measurement for the Kalman filter, which had seven outputs: three angular rates and four components of a quaternion. As a result, the output equations were linear. The partial derivatives were total derivatives and had constant values. The convergence algorithm replaced the computation of the

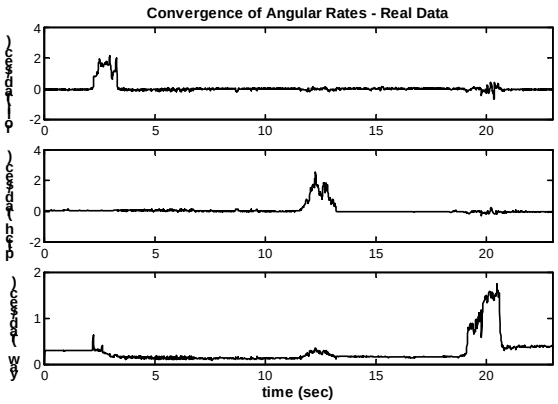

Figure 9. Tracking Results of Angular Rates Using Actual Data from the MARG Sensor.

iterations. The filter implementation used the Gauss-Newton algorithm because it does not involve second order derivatives.

The filter achieved excellent results for all tests using ideal synthetic data and actual sensor data. The convergence to the steady-state values took only three or four iteration steps. The filter is able to track rotational motion of the body on which the MARG sensor is attached. No singularities were observed, even when two consecutive 90-degree rotations were applied. Currently, fifteen MARG sensors are integrated to build a body suit that will be able to track posture of a person in virtual reality applications.

Although the authors's interest in quaternion based filter has thus far been restricted to human body motion

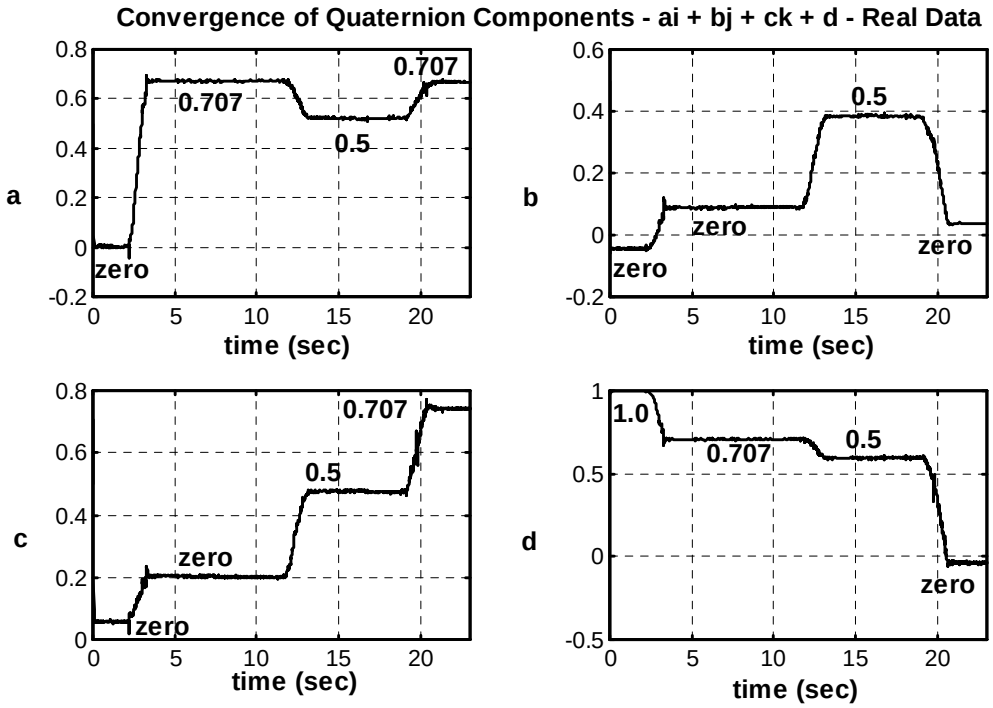

Figure 10. Tracking Results of Quaternion Components Using the Actual Data from the MARG Sensor.

partial derivatives of the nine nonlinear measurement equations. The computational requirements for the Kalman filter developed using this approach were significantly reduced, making it possible to estimate attitude in real time.

Extensive tests were conducted to verify the convergence of Gauss-Newton and Newton algorithms, and the performance of the Kalman filter. In almost all cases and for both Gauss-Newton and Newton algorithms, the convergence occurred in three or four

tracking, the approaches described above are also applicable to any highly maneuverable vehicle or robot. In particular, a similar problem without rate sensors has been investigated for application to manned or unmanned aircraft orientation estimation [17].

Acknowledgment

This work was in part supported by the Army Research Office (ARO) and the U.S. Navy Modeling and Simulation Office (N6).

References

1. Fakespace Labs, Inc., Mountain View, California, http://www.fakespace.com/products/boom3c.html.
2. Raab, F., Blood, E., Steiner, O., and Jones, H., "Magnetic Position and Orientation Tracking System," *IEEE Transactions on Aerospace and Electronics Systems*, AES-15, No. 5, 1979, pp. 709-717.
3. Welch, G., Bishop, G., Vicci, L., Brumback, S., Keller, L., Colucci, D., "The HiBall Tracker: High-Performance Wide-Area Tracking for Virtual and Augmented Environments," *Proceedings of the ACM Symposium on Virtual Reality Software and Technology 1999 (VRST 99*), University College London, 1999.
4. Vicon Motion Systems, http://www.metrics.co.uk/, Oxford Metric Ltd., Oxford, England.
5. Fuchs, E., *Inertial Head-Tracking*, Master's Thesis, Massachusetts Institute of Technology, Cambridge MA, 1993.
6. Foxlin, E., "Inertial Head-Tracker Sensor Fusion by a Complementary Separate-Bias Kalman Filter," *Proceedings of VRAIS* `96, IEEE, 1996, pp. 185-194.
7. Hayward, Roger C., Gebre-Egziabher, Demoz, Powell, J. David. *GPS-Based Attitude for Aircraft*. http://einstein.stanford.edu/gps/ABS/att_for_aircraft_rch1998.html (15 April 2000).
8. Quine, Ben. *Attitude Determination Subsystem*. http://www.atmosp.physics.utoronto.ca/people/ben/pages/spacecraft/Attitude.html (03 June 2000).
9. Leader, D.E., *Kalman Filter Estimation of Underwater Vehicle Position and Attitude Using a Doppler Velocity Aided Inertial Motion Unit*, Engineer Degree Thesis, Massachusetts Institute of Technology and Woods Hole Oceanographic Institution, Massachusetts, September 1994.
10. Bachmann, E. R., Duman, I., Usta, U. Y., McGhee, R.B., Yun, X. P., Zyda, M. J., "Orientation Tracking for Humans and Robots Using Inertial Sensors," *Proc. of 1999 Symposium on Computational Intelligence in Robotics & Automation*, Monterey, CA, November 1999.
11. Savage, P. G., *Strapdown Inertial Navigation Lecture Notes*, Strapdown Associates, Inc., Minnetonka, Minnesota 1985.
12. Kuipers, J.B., *Quaternions and Rotation Sequences*, Princeton University Press, Princeton, New Jersey 1999.
13. Brown, R.G. and Hwang, P.Y.C., *Introduction to Random Signals and Applied Kalman Filtering*, 3rd Edition, John Wiley and Sons, New York 1997.
14. Hagan, Martin T., Demuth, Howard B., Beale, Mark, *Neural Network Design*, PWS Publishing Company, Boston 1995.
15. Marins, J. L., An Extended Kalman Filter for Quaternion-Based Attitude Estimation, Engineer Degree's Thesis, Naval Postgraduate School, Monterey, California, September 2000.
16. McGhee, R.B., Bachmann, E.R., Yun, X., and Zyda, M.J., "Real-Time Tracking and Display of Human Limb Segment Motions Using Sourceless Sensors and a Quaternion-Based Filtering Algorithm --- Part I: Theory," MOVES Academic Group Technical Report NPS-MV-01-001, Naval Postgraduate School, Monterey, CA, November 2000.
17. Gebre-Egziabher, Demoz, Elkaim, Gabriel, Powell, J.D., and Parkinson, Bradford, "A Gyro-Free Quaternion-Based Attitude Determination System Suitable for Implementation Using Low Cost Sensors," Proceedings of IEEE 2000 Position Location and Navigation Symposium, March 13-16, 2000, pp. 185-192.